Synthesis and Design of Generalized Strongly Coupled Resonator Quartet Combline Filters with Redundant Resonance

Xiong Zhi'ang[1], Fan Jiyuan[1], Zhao Ping[1], Zhou Jinzhu[1], Shen Nan[2], Wu Qingqiang[2]

(1. Xidian University, Xi'an 710071, China;
2. ZTE Corporation, Shenzhen 518057, China)

DOI: 10.12142/ZTECOM.202601012

https://kns.cnki.net/kcms/detail/34.1294.TN.20260210.1137.004.html, published online February 10, 2026

Manuscript received: 2024-03-20

Abstract: This article proposes a generalized strongly coupled resonator quartet (GSCRQ) filter along with its synthesis approach. By introducing out-of-band reflection zeros (RZs), the proposed GSCRQ can generate a transmission zero on each side of the passband without negative couplings. The coupling coefficients in this coupling structure change with the positions of the out-of-band RZs. Thus, the GSCRQ configuration admits flexible design solutions. For GSCRQ coaxial combline filters, all couplings can be implemented as inductive couplings, simplifying the design and manufacturing process. In this article, a 6-2 filter in the GSCRQ configuration is synthesized and designed. The simulated results of the designed filter agree very well with the theoretical characteristics.

Keywords: filter synthesis; generalized strongly coupled resonator quartets (GSCRQ); out-of-band reflection zero; transmission zero

Citation (Format 1): Xiong Z A, Fan J Y, Zhao P, et al. Synthesis and design of generalized strongly coupled resonator quartet combline filters with redundant resonance [J]. ZTE Communications, 2026, 24(1): 88 - 98. DOI: 10.12142/ZTECOM.202601012

Citation (Format 2): Z. A. Xiong, J. Y. Fan, P. Zhao, et al. "Synthesis and design of generalized strongly coupled resonator quartet combline filters with redundant resonance," *ZTE Communications*, vol. 24, no. 1, pp. 88 - 98, Mar. 2026. doi: 10.12142/ZTECOM.202601012.

1 Introduction

Transmission zeros (TZs) at finite frequencies are commonly seen in modern microwave filters. They can improve frequency selectivity and out-of-band rejection of bandpass filters. Nowadays, cross-couplings are the most commonly used method to realize TZs. Frequently used cross-coupled structures include trisections, quartets, and box sections[1-3]. Cross-coupled configurations generate TZs by multi-path cancellation. TZs are generated when the combined signals interfere destructively at the combining node. A trisection or a box section can realize only one TZ on the imaginary axis. A quartet can introduce two TZs, and the two TZs can be on the imaginary axis or form a para-conjugate pair. Usually, when the generalized Chebyshev filter has TZs on the lower side of the passband, at least one of the couplings in the trisection or quartet has to be negative. Negative couplings in coaxial combline filters are often realized by capacitive probes. The capacitive probe increases complexity, reduces power handling capability, and is inconvenient for post-production tuning.

Macchiarella et al. proposed strongly coupled resonator pairs (SCRP)[4] and strongly coupled resonator triplets (SCRT)[5]. Compared with traditional filters, strongly coupled filter configurations consist solely of positive couplings, even though TZs on the lower stopband are realized. It is also interesting to note that there is a reflection zero (RZ) in the lower stopband. Zeng[6] introduced an out-of-band RZ into the synthesis of equi-ripple filtering functions, enabling the SCRT structure to be synthesized directly by coupling matrix transformations. This synthesis approach addresses the limitation that the out-of-band RZ of the SCRT must be designed far from the passband. The synthesized structure is named the generalized strongly coupled resonator triplet (GSCRT). Recently, a coaxial combline filter design was proposed based on the strongly coupled resonator quadruplet (SCRQ)[7]. The SCRQ consists of an SCRT and a regularly coupled fourth resonator. However, there is no analytical synthesis method

This work was supported by the National Natural Science Foundation of China under Grant No. 62471366.

for SCRQ filters.

This work presents the synthesis and design of a generalized strongly coupled resonator quartet (GSCRQ), where all couplings can be positive, as determined by the synthesis procedure. Compared with SCRQ, GSCRQ can arbitrarily specify the location of the out-of-band RZ to achieve a flexible topology configuration. First, the working mechanism of GSCRQ at the circuit level is analyzed, and the relationship between the TZs and couplings (self-coupling and mutual coupling) is explained. Then, a direct matrix synthesis approach for filters with GSCRQ is presented. In addition, this paper proposes a parameter-extraction method for filters with out-of-band RZs. The method can aid the design and tuning process of filters with GSCRQ. The filter-tuning process is faster than port-tuning[8]. Finally, a sixth-order filter with a GSCRQ is synthesized and the simulation results show good agreement with the synthesized response.

2 Filters with GSCRQ

In order to understand the working mechanism of the GSCRQ configuration, we first analyze the circuit model of the quartet shown in Fig. 1. The TZs are generated by the couplings among resonators 1 – 4. The admittance matrix $\boldsymbol{Y}$ between nodes 1 and 4 is

$$\begin{aligned}\boldsymbol{Y} = &\frac{1}{s+\mathrm{j}B_2}\begin{bmatrix} M_{12}^{\ 2} & M_{12}M_{24} \\ M_{12}M_{24} & M_{24}^2 \end{bmatrix} + \begin{bmatrix} 0 & \mathrm{j}M_{14} \\ \mathrm{j}M_{14} & 0 \end{bmatrix} + \\ &\frac{1}{s+\mathrm{j}B_3}\begin{bmatrix} M_{13}^{\ 2} & M_{13}M_{34} \\ M_{13}M_{34} & M_{34}^2 \end{bmatrix} = \\ &\frac{1}{(s+\mathrm{j}B_2)(s+\mathrm{j}B_3)} \times \\ &\begin{bmatrix} \cdots & (M_{12}M_{24}+\mathrm{j}M_{14}s-B_2M_{14})(s+\mathrm{j}B_3)+(s+\mathrm{j}B_2)(M_{13}M_{34}) \\ \cdots & \cdots \end{bmatrix}\end{aligned} \tag{1}$$

Equating the numerator polynomial of Y_{12} to zero, we can identify the TZs generated by the GSCRQ as:

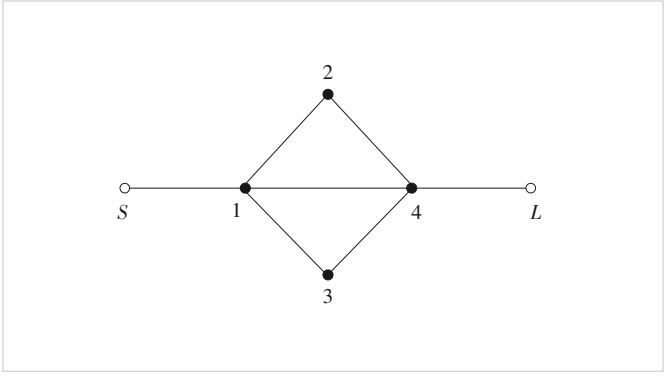

Figure 1. Topology of quartets. Black nodes represent resonators, and solid lines represent couplings

$$\begin{aligned}s_{\mathrm{TZ}} = &\frac{\mathrm{j}}{2M_{14}} \times \\ &\left(\begin{array}{c} \left(M_{12}M_{24}+M_{13}M_{34}-M_{14}\left(B_2+B_3\right)\right) \pm \\ \sqrt{\left(M_{12}M_{24}-B_2M_{14}-B_3M_{14}+M_{13}M_{34}\right)^2 + \\ 4M_{14}\left(B_3M_{12}M_{24}-B_3B_2M_{14}+B_2M_{13}M_{34}\right)} \end{array} \right)\end{aligned} \tag{2}$$

Empirically, for the quartet shown in Fig. 1, whether the TZs are located in the upper or lower stopband, there will exist a negative coupling. According to Eq. (2), it can be seen that the mutual couplings and self-couplings interact with each other to generate two TZs. We consider introducing out-of-band RZs to realize TZs while keeping all the couplings in the quartet positive.

2.1 Remez-Like Algorithm

Lowpass prototype filter responses can be defined as the ratio of polynomials $E(s)$, $F(s)$, $F_{22}(s)$ and $P(s)$ as:

$$\boldsymbol{S} = \frac{1}{E(s)}\begin{bmatrix} F(s)/\varepsilon_R & P(s)/\varepsilon \\ P(s)/\varepsilon_R & F_{22}(s)/\varepsilon_R \end{bmatrix} \tag{3}$$

where ε and ε_R are positive real constants such that the absolute values of the highest-order coefficients in $E(s)$, $F(s)$, $F_{22}(s)$ and $P(s)$ can be normalized.

To synthesize a filter with out-of-band RZs, a Remez-like iterative algorithm can be used. The polynomials $F_{\mathrm{out}}(\omega)$, $F_{\mathrm{in}}(\omega)$, and $P(\omega)$ are defined as:

$$F_{\mathrm{out}}(\omega) = \prod_{i=1}^{nc}\left(\omega - \omega_{\mathrm{out},i}\right) \tag{4a}$$

$$F_{\mathrm{in}}(\omega) = \prod_{i=1}^{np-nc}\left(\omega - \omega_{\mathrm{in},i}\right) \tag{4b}$$

$$P(\omega) = \prod_{i=1}^{nz}\left(\omega - \omega_{nz}\right) \tag{4c}$$

where np is the order of the filter, nc is the number of out-of-band RZs, $\omega_{\mathrm{in},i}$ denotes in-band RZs, ω_{nz} and $\omega_{\mathrm{out},i}$ are the assigned TZs and out-of-band RZs, respectively. In the Remez-like algorithm, $F_{\mathrm{out}}(\omega)$ is completely determined by the assigned out-of-band RZs. We seek the $np-nc$ unknown coefficients $\{a_i\}$ of $F_{\mathrm{in}}(\omega)$ such that the characteristic function $C(\omega)=F_{\mathrm{out}}(\omega)F_{\mathrm{in}}(\omega)/P(\omega)$ is equiripple in the passband. The filtering synthesis procedure then proceeds as follows.

Step 1: Solve the linear system comprising $np-nc+1$ equations with the $np-nc+1$ unknowns $\left[\{a_i\},\Delta\right]$:

$$\begin{cases} C(-1) = \Delta \\ C\left(\Omega_k\right) = (-1)^k\Delta \quad k = 1,\cdots,np-nc-1 \\ C(1) = (-1)^{np-nc}\Delta \end{cases} \tag{5}$$

where Δ is the amplitude of the in-band ripple of $C(\omega)$ and Ω_k are the extreme points. The equations in Eq. (5) can be re-written in a matrix form as:

$$\begin{bmatrix} \Omega_1^{np-nc-1} & \Omega_1^{np-nc-2} & \cdots & 1 & -P(\Omega_1)/F_{out}(\Omega_1) \\ \Omega_2^{np-nc-1} & \Omega_2^{np-nc-2} & \cdots & 1 & P(\Omega_1)/F_{out}(\Omega_2) \\ \vdots & \vdots & \vdots & \vdots & \vdots \\ \Omega_{np+1}^{np-nc-1} & \Omega_{np+1}^{np-nc-2} & \cdots & 1 & (-1)^{np-nc+1}P(\Omega_1)/F_{out}(\Omega_1) \end{bmatrix} \begin{bmatrix} a_{np-nc-1} \\ a_{np-nc-2} \\ \vdots \\ a_0 \\ \Delta \end{bmatrix} = \begin{bmatrix} -\Omega_1^{np-nc} \\ -\Omega_2^{np-nc} \\ \vdots \\ -\Omega_{np+1}^{np-nc} \end{bmatrix} \quad (6),$$

where a_i ($i = np-nc-1, \cdots, 0$) are the coefficients of the polynomial $F_{in}(\omega)$.

Step 2: After obtaining the coefficients a_i, update the locations of the in-band extrema Ω' by solving $(\partial C(\omega)/\partial\omega) = 0$.

Step 3: Repeat Steps 1 and 2 until convergence is achieved, i.e., $|\Omega - \Omega'|$ is sufficiently close to zero. At convergence, the coefficients $\{a_i\}$ of $F_{in}(\omega)$ are stable. The polynomial $F(\omega)$ is then constructed as:

$$F(\omega) = F_{in}(\omega)F_{out}(\omega) \quad (7).$$

Step 4: Calculate ε and ε_R using

$$\varepsilon_R = 1, \quad \varepsilon = \frac{1}{\sqrt{10^{RL/10}-1}}\left|\frac{P(\omega)}{F(\omega)}\right|_{\omega=\pm1} \quad (8),$$

where RL is the desired return loss level.

The monic polynomial $E(\omega)$ is obtained from $P(\omega)$ and $F(\omega)$ through the Feldtkeller equation:

$$E(\omega)E(\omega)^* = F(\omega)F(\omega)^*/\varepsilon_R^2 + P(\omega)P(\omega)^*/\varepsilon^2 \quad (9).$$

We can solve the right-hand side of Eq. (9) to obtain $2np$ roots, from which those with positive imaginary parts are selected to construct $E(\omega)$. Alternatively, a more robust computational method has been recently proposed in Ref. [9] to accurately solve the Feldtkeller equation for high-order networks. After $E(\omega)$ is obtained, the polynomials $F(s)$, $P(s)$ and $E(s)$ are formed by the variable substitution $\omega = s/j$. If the coefficients of the highest order terms of these polynomials, obtained by variable substitution, are not equal to 1, they should be normalized by dividing the coefficient of the highest order terms. It should be noted that when $np-nc$ is even, $P(s)$ is multiplied by j to satisfy the unitary condition, ensuring its highest-order coefficient is j[10]. Finally, the polynomial $F_{22}(s)$ is given by

$$F_{22}(s) = (-1)^{np}F(s)^* \quad (10),$$

where (*) denotes polynomial para-conjugation.

After the Chebyshev-like polynomials are synthesized, the $np + 2$ transversal coupling matrix can be synthesized using the well-established technique described in Ref. [10]. The GSCRQ coupling topology is then obtained by a sequence of similarity transformations from the transversal coupling matrix.

The synthesis process properties of GSCRQ will be demonstrated and discussed in the following sections.

2.2 A Synthesis Example of GSCRQ Filters

Consider an example with $np = 7$ poles, $nc = 1$ out-of-band RZ, and TZs at $\{s_{TZ}\} = \{-1.36j, 1.25j\}$. The return loss level is RL = 20 dB, and the assigned out-of-band RZ is $s_{out} = -8.26j$.

First, $P(\omega)$ and $F_{out}(\omega)$ are obtained from the prescribed TZs and the out-of-band RZ, respectively:

$$P(\omega) = (\omega + 1.36)(\omega - 1.25) = \omega^2 + 0.11\omega - 1.7 \quad (11a),$$

$$F_{out}(\omega) = \omega + 8.26 \quad (11b).$$

We begin with an initial guess that positions of in-band extrema $\{\Omega_k\}$ are evenly distributed over $[-1, 1]$ rad/s; thus, the initial set is $\Omega = [-1, -2/3, -1/3, 0, 1/3, 2/3, 1]$. In practice, we can arbitrarily choose $N-1$ (where N is the filter order) different extrema within $(-1, 1)$, and our experiments show that the proposed method converges to the correct result. Solving Eq. (6) yields the function $F_{in}(\omega)$ as:

$$F_{in}(\omega) = \omega^6 - 0.028\,5\omega^5 - 1.418\,2\omega^4 + 0.032\,9\omega^3 + 0.442\,5\omega^2 - 0.006\,3\omega - 0.017\,1 \quad (12).$$

By solving $(\partial C(\omega)/\partial\omega) = 0$, we obtain updated positions of in-band extrema: $\Omega' = [-6.595\,2, -1.592\,7, -0.879\,5, -0.444\,8, 0.011\,0, 0.463\,9, 0.893\,3, 1.426\,8]$. Then, the five frequencies lying within the passband are selected and, together with the two band edge frequencies -1 and 1, form the seven extremal points for the next iteration: $\Omega = [-1, -0.879\,5, -0.444\,8, 0.011\,0, 0.463\,9, 0.893\,3, 1]$ rad/s. This process is repeated for 10 iterations, after which the extremal locations converge to stable values. Meanwhile, the coefficients $\{a_i\}$ of $F_{in}(\omega)$ are determined. Fig. 2 shows the results of the first four iterations. It can be found that $C(\omega)$ is stable in the fourth iteration. Then, $F(\omega)$ and ε are calculated using Eqs. (7) and (8), respectively. $E(\omega)$ is solved from the Feldtkeller equation. Finally, $F(\omega)$, $P(\omega)$, and $E(\omega)$ are transformed into $F(s)$, $P(s)$, and $E(s)$. The coefficients of the final polynomials are listed in Table 1, and the filter response is shown in Fig. 3.

A transversal coupling matrix is synthesized from the polynomials. Then, the coupling topology shown in Fig. 4a is obtained through a series of rotation transformations (Table 2). Specifically, Steps 1 – 21 synthesize an "arrow" topology, while Steps 22 – 30 form a quartet among nodes 2 to 5. In

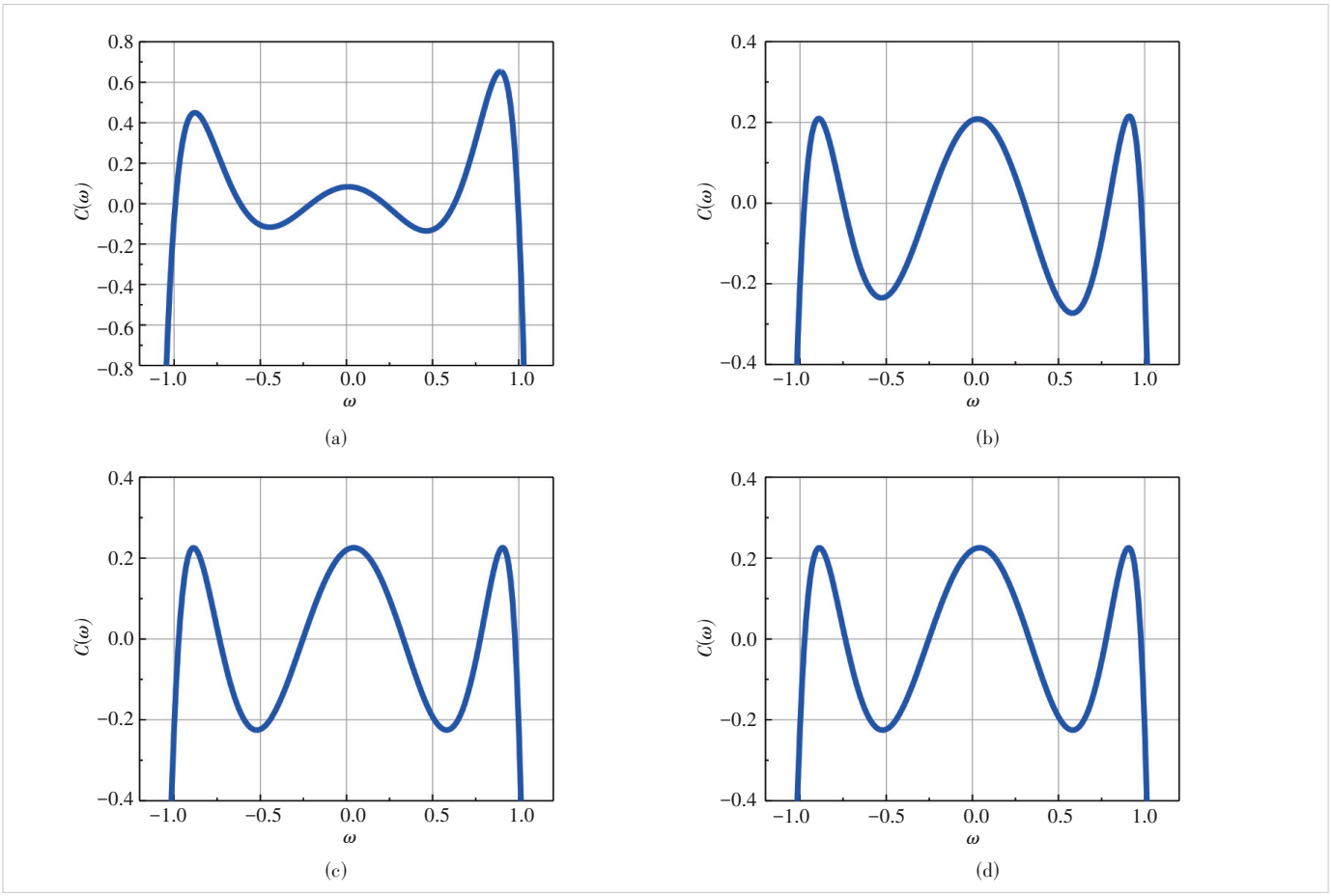

Figure 2. Iterations of Remez-like algorithm in solving the equi-ripple function for the 7th-order filter with an out-of-band RZ: (a) the first iteration; (b) the second iteration; (c) the third iteration; (d) the fourth iteration

Table 1. Coefficients of $F(s)$, $P(s)$, and $E(s)$ of seven-poles with one upper TZ and one lower TZ

s^i, i =	$F(s)$ ($F_{22}(s)$)	$P(s)$	$E(s)$
0	0.373 8j	1.700 0	0.868 3 + 3.731 5j
1	0.422 9	0.110 0j	2.769 1 +12.801 1j
2	5.464 5j	1.000 0	4.956 1 + 24.638 4j
3	2.012 0		6.466 5 + 30.408 0j
4	13.070 5j		5.796 9 + 28.889 2j
5	2.613 9		4.560 8 + 16.045 3j
6	8.137 5j		1.973 3 + 8.137 5j
7	1.000 0		1.000 0
ε_R = 1.000 0		ε = 0.445 8	

TZ: transmission zero

Fig. 4, the numerical values without underscores represent mutual and I/O couplings, whereas those with underscores denote self-couplings. Notably, all mutual coupling values are positive. Therefore, in the physical implementation, all the inter-resonator couplings can be realized as inductive couplings.

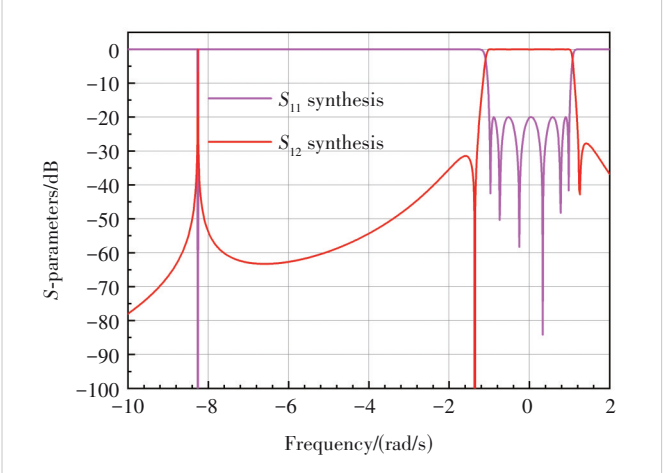

Figure 3. Synthesized response of the 7th-order filter with an out-of-band RZ

2.3 Impact of Out-of-Band RZ

To observe the impact of out-of-band RZ on the filter response, we compare the proposed 7th-order RZ filter (Fig. 4a)

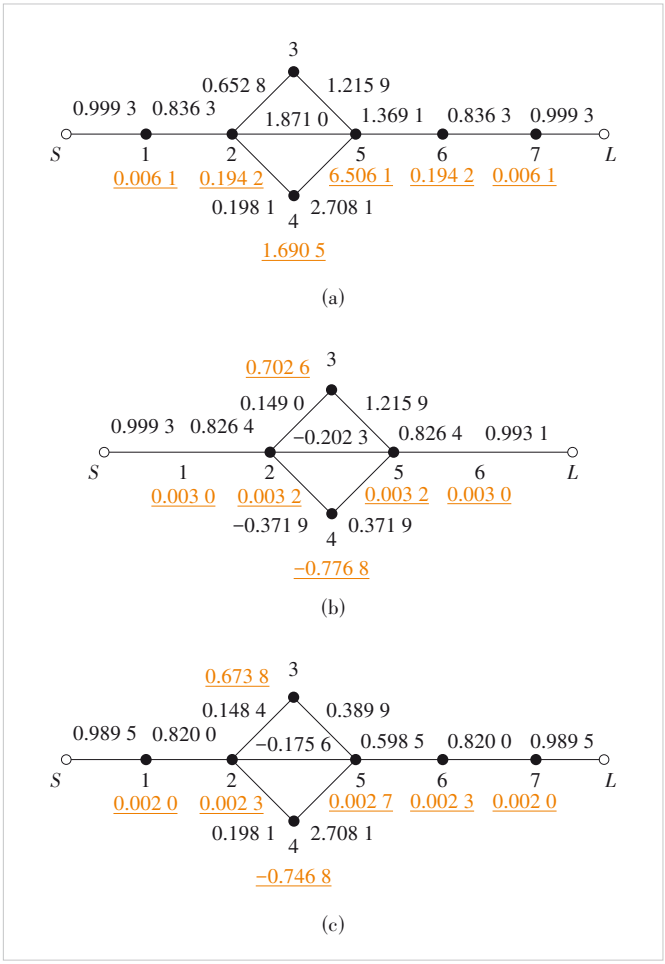

Figure 4. Topology with quartet: (a) 7-2 (7 RZs and 2 TZs) filter with an out-of-band RZ; (b) 6-2 filter; (c) 7-2 filter

Table 2. Rotation sequence to the filter in Fig. 4a

Rotation sequence	Elements to be annihilated	Pivot [i, j]	Rotation sequence	Elements to be annihilated	Pivot [i, j]
1	M_{S7}	[7, 6]	16	M_{37}	[7, 6]
2	M_{S6}	[6, 5]	17	M_{36}	[6, 5]
3	M_{S5}	[5, 4]	18	M_{35}	[5, 4]
4	M_{S4}	[4, 3]	19	M_{47}	[7, 6]
5	M_{S3}	[3, 2]	20	M_{46}	[6, 5]
6	M_{S2}	[2, 1]	21	M_{57}	[7, 6]
7	M_{17}	[7, 6]	22	M_{5L}	[5, 6]
8	M_{16}	[6, 5]	23	M_{6L}	[6, 7]
9	M_{15}	[5, 4]	24	M_{46}	[5, 6]
10	M_{14}	[4, 3]	25	M_{47}	[4, 5]
11	M_{13}	[3, 2]	26	M_{57}	[5, 6]
12	M_{27}	[7, 6]	27	M_{35}	[4, 5]
13	M_{26}	[6, 5]	28	M_{36}	[3, 4]
14	M_{25}	[5, 4]	29	M_{46}	[4, 5]
15	M_{24}	[4, 3]	30	M_{34}	[3, 4]

with two traditional counterparts: a 6th-order filter and a 7th-order filter (Figs. 4b and 4c). The TZs for all three filters are set at $\{s_{TZ}\} = \{-1.36j, 1.25j\}$, with a specified return loss of 20 dB. The key difference lies in their synthesis procedures and the resulting coupling matrices. In the traditional filters, the absolute values of coupling coefficients are all less than 1. In contrast, the proposed filter with an out-of-band RZ has couplings greater than 1. Couplings with normalized coupling coefficients exceeding 1 are defined as strong couplings. The quartet possessing such strong couplings constitutes a GSCRQ. Realizing strong coupling between resonant rods requires reducing the distance between adjacent resonant rods. This close arrangement is beneficial for the miniaturization of coaxial combline filters.

The introduction of out-of-band RZ affects not only the coupling coefficients but also the filter's response. Fig. 5 compares the responses of the three filters in Fig. 4. The 7th-order GSCRQ filter with an out-of-band RZ exhibits in-band characteristics similar to the conventional 6th-order filter, but its lower stopband rejection is worse than that of the 6th-order filter. In addition, its upper stopband rejection is slightly better than that of the 6th-order filter but remains worse than that of the seventh-order filter.

The above analysis confirms that an out-of-band RZ affects both the coupling coefficients and filter characteristics. This introduces additional flexibility into the filter synthesis. To demonstrate this, the location of the out-of-band RZ in the 7th-order filteris varied to −3.5 rad/s or −6.7 rad/s. Fig. 6 compares the frequence responses for the original RZ at −8.26 rad/s, −3.5 rad/s, and −6.7 rad/s with these two new locations. The corresponding coupling matrices are given in Fig. 7. Fig. 6 shows that when the out-of-band RZ is closer to the passband, the out-of-band suppression in the near passband will be

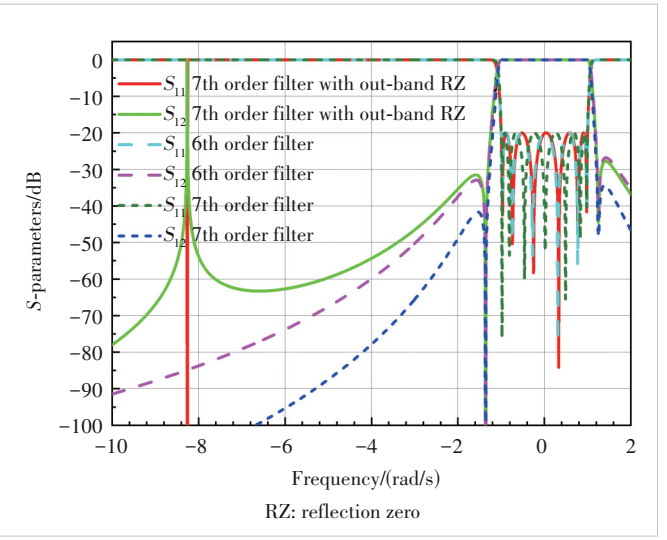

Figure 5. Frequency responses of three filter designs: the 7th-order filter with an out-of-band reflection zero (solid), 6th-order traditional filter (dashed), and 7th-order traditional filter (dotted)

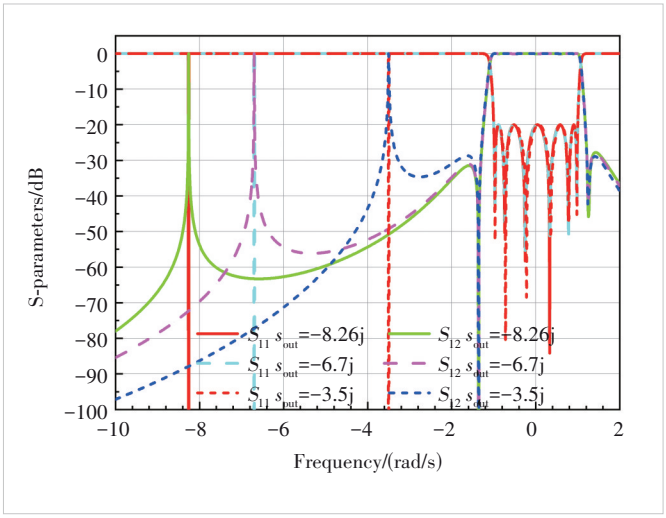

Figure 6. Frequency responses with different out-of-band RZ locations: s_{out} = −8.26j (solid), s_{out} = −6.7j (dashed), and s_{out} = −3.5j (dotted)

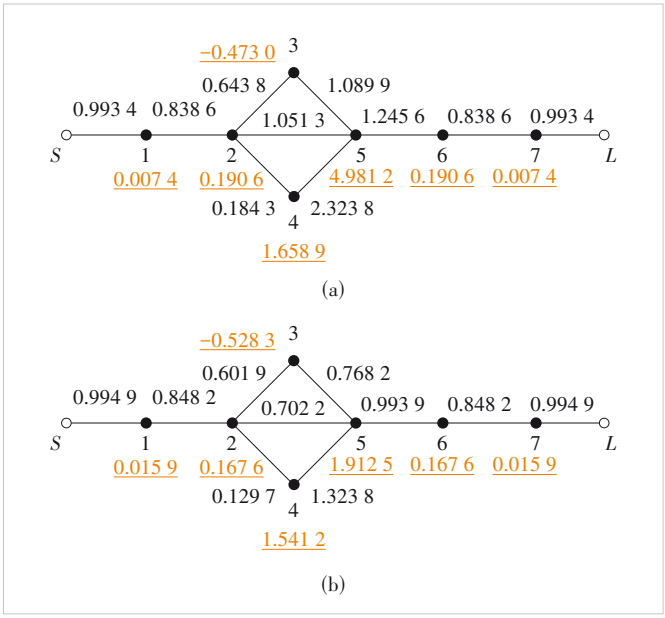

Figure 7. 7-2 filter topology with different out-of-band RZ locations: (a) s_{out} = −6.7j; (b) s_{out} = −3.5j

worse, and the couplings in the quartet become weaker. Therefore, in the actual filter design, we can tune the position of the out-of-band RZ to meet the design specifications. However, it should be noted that placing the out-of-band RZ too far from the passband results in excessively strong mutual coupling in the GSCRQ, making it difficult to realize in practice.

3 Design Example

To validate the synthesis method, a 6th-order bandpass filter using coaxial resonators is designed. Its physical layout and the coupling topology are shown in Figs. 8a and 8b, respectively. The key design specifications include a center frequency f_0 = 2.5 GHz and a bandwidth BW = 200 MHz.

In previous literature, the design of strongly coupled resonator filters is often performed using the "port tuning" technique[11]. This field-circuit co-simulation method uses circuit optimization to tune the filter, which typically requires only a few seconds. In addition, due to dispersion and capacitive loading effects of the resonant rods, a large difference exists between the out-of-band resonance of the simulated response and the ideal response. To make the ideal response consistent with the simulated response, it is generally necessary to optimize a target matrix that takes stray couplings into account. For strongly coupled resonator filters, we propose a novel Model-Based Vector Fitting (MVF)-based method to achieve tuning of strongly coupled filters[12 − 13]. The procedure includes the following five steps:

Step 1: Map the physical frequency to the low-pass domain:

$$\omega = \frac{f_0}{\mathrm{BW}}\left(\frac{f}{f_0} - \frac{f_0}{f}\right) \tag{13},$$

where f_0 and BW are the center frequency and bandwidth of the filter, respectively.

Step 2: De-embed the phase from the simulated *S*-parameters by vector fitting[11].

Step 3: Transform phase-corrected *S*-parameter to *Y*-parameter, and use MVF to approximate the *Y*-parameter data[10].

Step 4: Synthesize a transversal coupling matrix from the *Y*-parameter rational functions and transform it to the target form.

Step 5: Compare extracted and ideal synthesized matrices, and adjust the dimensions of the filter accordingly.

The second step is crucial for identifying the true poles and zeros of the coupled resonator filter. In a traditional single-passband filter, plotting the poles and zeros of the reflection coefficient on the complex s-plane reveals that most of the poles and zeros cluster around the origin, whereas a few are located far away. Those near the origin are contributed by the resonators, while the distant ones result from phase loading and feed lines[13]. Empirically, for traditional single-passband filters, poles and zeros located beyond four units from the origin are caused by phase loading and feed lines. However, this rule does not apply to strongly coupled resonator filters. Let us take the simulated reponses of the EM model in Fig. 8 as an example. Vector fitting (VF) is applied to S_{11} to obtain an optimal rational approximation. The zeros and poles of the fitting rational functions are listed in Table 3.

If zeros and poles more than four units from the origin (i.e., the 6th, 7th, and 8th in Table 3) are selected to construct the phase factor, a spike appears in its amplitude near −11.5 rad/s, as shown in Fig. 9a. This indicates erroneous phase de-embedding, as the amplitude and phase of the phase factor should be smooth. Corresponding errors are also observed in the de-embedded phase of S_{11} or S_{22}. As shown in Fig. 9b, the

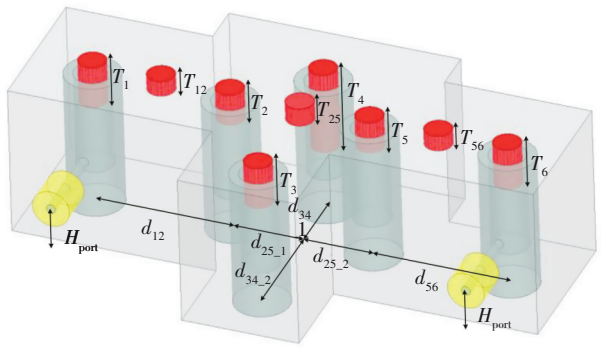

(a)

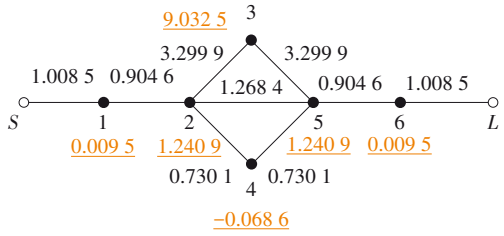

Note: The numerical values with underscores are self-couplings, while the numerical values without underscores are mutual couplings and I/O couplings.

(b)

Figure 8. (a) Electromagnetic model of the 6th-order filter with GSCRQ; (b) synthesis results of GSCRQ of the 6-2 filter with one out-of-band RZ

Table 3. Zeros and poles of VF results for S_{11}

k	poles	zeros
1	−0.692 7 + 0.104 7i	0.001 0 + 0.072 2i
2	−0.556 11−0.675 5i	−0.000 1−0.530 2i
3	−0.481 2 + 0.805 7i	−0.000 5 + 0.657 6i
4	−0.180 53−1.073 5i	−0.000 7−0.889 7i
5	−0.156 41 + 1.149 1i	0.000 3 + 1.000 2i
6	−0.009 1−11.503 2i	0.000 0−11.503 1i
7	1.132 2 + 14.087 9i	1.664 5 + 13.927 9i
8	−26.468 1 + 3.616 4i	26.542 8 + 3.463 7i

phases of S_{11} and S_{22} are very smooth in the lower stopband, which is correct for traditional filters. However, for a strongly coupled resonator filter with an out-of-band RZ, the phases of S_{11} and S_{22} should exhibit abrupt changes, not smoothness. Therefore, we speculate that the wrong phase factor offsets the original mutation, making the phases of S_{11} and S_{22} smooth after phase de-embedding.

To obtain the correct phase factor, the 6th pole-zero pair is attributed to the filter itself rather than to phase loading and transmission lines, yielding the phase factor shown in Fig. 10a. The phase no longer changes suddenly around − 11.5 rad/s,

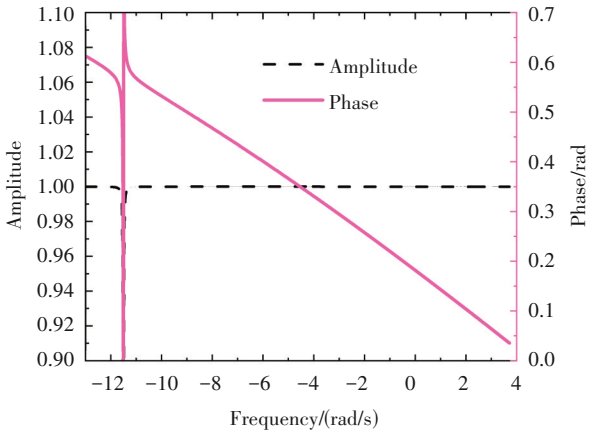

(a)

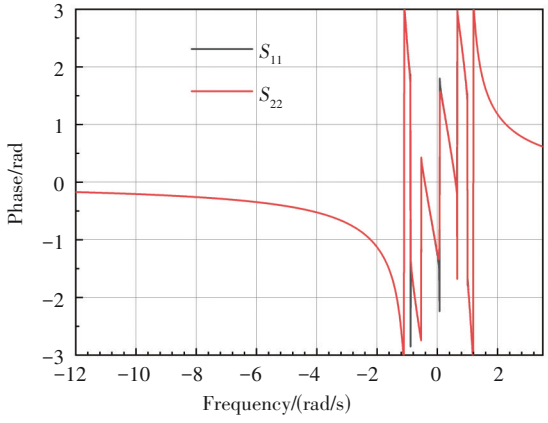

(b)

Figure 9. Incorrect phasing de-embedding: (a) amplitude and phase of the phase factor α; (b) S_{11} and S_{22} after phase removal

which proves that this phase factor is physically consistent. In addition, Fig. 10 shows the S-parameter phase after phase de-embedding, where the out-of-band RZ now correctly appears at − 11.5 rad/s. Based on extensive experiments, we recommend that for strongly coupled filters, the threshold for phase de-embedding is set to

$$\text{Thresh} = \min(s_{\text{out}}) - 1 \quad (14),$$

where $\min(s_{\text{out}})$ is the minimum out-of-band RZ.

After phase de-embedding, MVF is used to fit a 7th-order polynomial of the Y-parameters (Step 3). A transversal coupling matrix is then synthesized and transformed to the target form (Step 4). By comparing the extracted and ideal synthesized matrices, the filter dimensions are adjusted accordingly (Step 5), enabling rapid tuning to meet the target specifications. The simulation results with ideal lossless materials are shown in Fig. 11, where dashed lines are simulation data, and solid lines are the ideal synthesis responses. The input

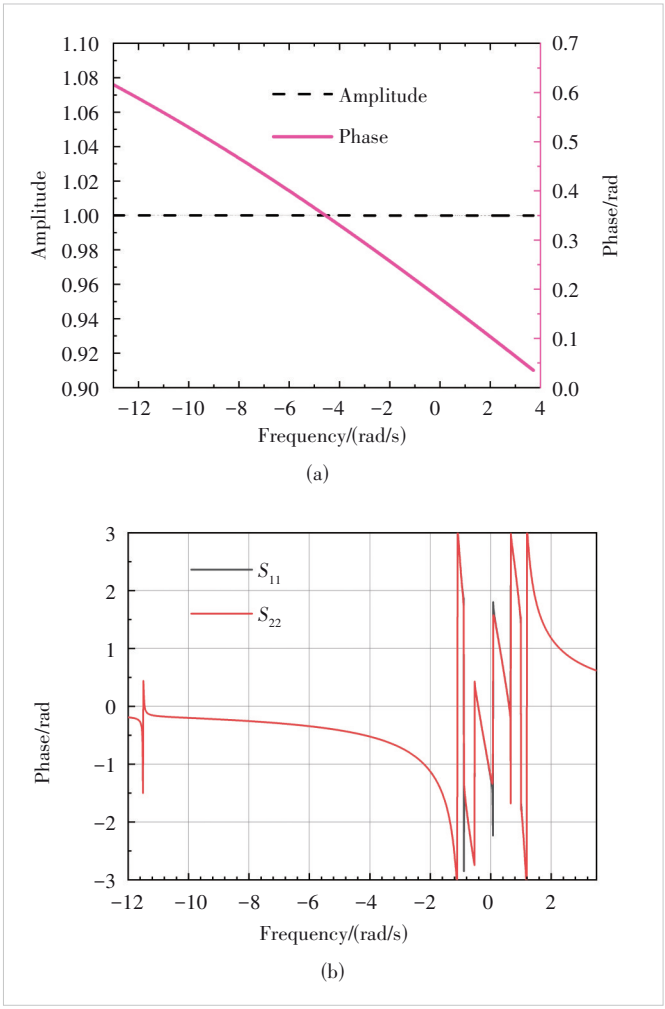

Figure 10. Correct phase de-embedding: (a) amplitude and phase of the phase factor α and (b) S_{11} and S_{22} after phase removal

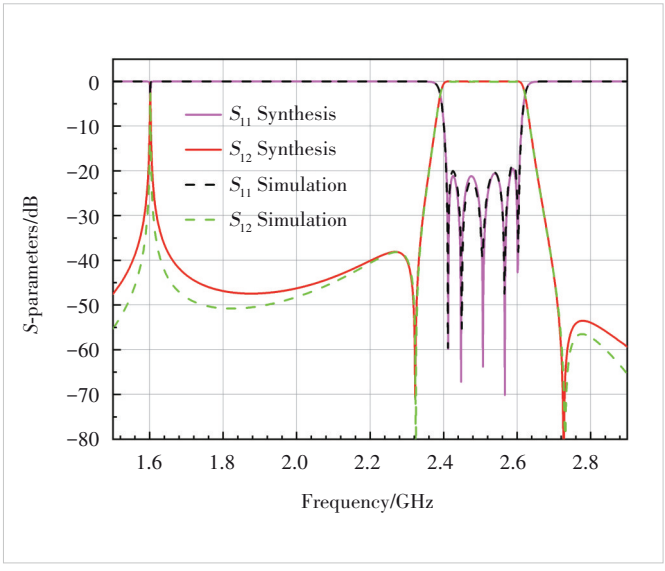

Figure 11. Simulated results using High Frequency Structure Simulator (HFSS) and ideal synthesis responses of the filter

feed comes from a coaxial cable whose inner and outer radii are 0.5 mm and 2 mm, respectively. The coaxial cable is filled with a dielectric with a relative permittivity ε_R = 2.2. The inner and outer radii of the resonant rods are 2 mm and 3 mm and the height of the enclosure box is 16.5 mm. Other detailed dimensions are shown in Table 4.

Table 4. Dimensions of the filter in Fig. 8

Resonator ID	T_1	T_2	T_3	T_4	T_5	T_6	T_{12}	T_{25}	T_{56}
Final/mm	4.70	3.55	9.10	4.7	3.55	4.70	1.70	2.00	2.00
Dimension	d_{12}	d_{25_1}	d_{25_2}	d_{34_1}	d_{34_2}	H_{port}			
Final/mm	1.77	7.55	7.55	6.40	11.43	6.32			

4 Conclusions

In this article, synthesis and design of filters with GSCRQs are presented. The GSCRQ enables the generation of two TZs without requiring negative couplings. Its work mechanism is analyzed based on a circuit model for the first time. A complete filter design procedure is demonstrated, including the coupling matrix synthesis and EM model tuning. The full-wave EM simulation results show excellent agreement with the theoretical predictions, thereby validating the theory of filters with GSCRQ.

References

[1] Levy R. Direct synthesis of cascaded quadruplet (CQ) filters [C]//Proc. 1995 IEEE MTT-S International Microwave Symposium. 1995: 497 - 500. DOI:10.1109/MWSYM.1995.406038
[2] Levy R, Petre P. Design of CT and CQ filters using approximation and optimization [J]. IEEE transactions on microwave theory and techniques, 2001, 49(12): 2350 - 2356. DOI:10.1109/22.971620
[3] Tamiazzo S, Macchiarella G. An analytical technique for the synthesis of cascaded N-tuplets cross-coupled resonators microwave filters using matrix rotations [J]. IEEE transactions on microwave theory and techniques, 2005, 53(5): 1693 - 1698. DOI:10.1109/TMTT.2005.847065
[4] Macchiarella G, Bastioli S, Snyder R V. Design of in-line filters with transmission zeros using strongly coupled resonators pairs [J]. IEEE transactions on microwave theory and techniques, 2018, 66(8): 3836 - 3846. DOI: 10.1109/TMTT.2018.2840981
[5] Bastioli S, Snyder R V, Macchiarella G. Design of in-line filters with strongly coupled resonator triplet [J]. IEEE transactions on microwave theory and techniques, 2018, 66(12): 5585 - 5592. DOI: 10.1109/TMTT.2018.2867004
[6] Zeng Y, Yang Y M, Yu M, et al. Synthesis of generalized strongly coupled resonator triplet filters by regulating redundant resonant modes [J]. IEEE transactions on microwave theory and techniques, 2022, 70(1): 864 - 875. DOI:10.1109/TMTT.2021.3128602
[7] Bastioli S, Snyder R V, Macchiarella G. The strongly coupled resonator quadruplet [J]. IEEE microwave and wireless technology letters, 2023, 33 (8): 1135 - 1138. DOI:10.1109/LMWT.2023.3270099
[8] Otto S, Lauer A, Kassner J, et al. Full wave coupled resonator filter optimization using a multi-port admittance-matrix [C]//2006 Asia-Pacific Microwave Conference. IEEE, 2006: 777 - 780. DOI:10.1109/APMC.2006.4429530
[9] Zhao P, Liu B Z, Oldoni M, et al. Improving accuracy in solving Feldtkeller equation [J]. IEEE microwave and wireless technology letters, 2024,

34(3): 251 – 254. DOI:10.1109/LMWT.2023.3349133
[10] Cameron R J, Kudsia C M, Mansour R R. Microwave filters for communication systems: fundamentals, design and applications [M]. 2nd ed. Hoboken: Wiley, 2018. DOI: 10.1002/9781119292371
[11] Seyfert F, Baratchart L, Marmorat J P, et al. Extraction of coupling parameters for microwave filters: determination of a stable rational model from scattering data [C]//IEEE MTT-S International Microwave Symposium Digest. IEEE, 2003: 25 – 28. DOI: 10.1109/MWSYM.2003.1210875
[12] Zhao P, Wu K L. Model-based vector-fitting method for circuit model extraction of coupled-resonator diplexers [J]. IEEE transactions on microwave theory and techniques, 2016, 64(6): 1787 – 1797. DOI: 10.1109/TMTT.2016.2558639
[13] Zhao P. Phase De-embedding of narrowband coupled-resonator networks by vector fitting [J]. IEEE transactions on microwave theory and techniques, 2023, 71(4): 1439 – 1446. DOI:10.1109/TMTT.2018.2854170

Biographies

Xiong Zhi'ang received his BS degree from Jiangxi University of Science and Technology, China in 2021, and the master's degree from Xidian University, Xi'an, China in 2024. His current research interests include mixed electric and magnetic coupling filters and modeling and optimization of microwave passive filters.

Fan Jiyuan received his BS degree from Nanjing University of Posts and Telecommunications, China in 2022 and his master's degree from Xidian University, China in 2025. His current research interests include mixed electric and magnetic coupling, as well as the synthesis and tuning of multiband filters and multiplexers.

Zhao Ping (aoing56@gmail.com) received his BS degree from Nanjing University, China in 2012, and PhD degree from The Chinese University of Hong Kong, China in 2017. From 2017 to 2019, he was a post-doctoral researcher with the École Polytechnique de Montréal, Canada. He joined the National Key Laboratory of Antennas and Microwave Technology, Xidian University, China in 2020. Since 2024, he has been with the State Key Laboratory of Electromechanical Integrated Manufacturing of High-performance Electronic Equipments, Xidian University, where he is currently an associate professor. His research interests include coupling matrix synthesis techniques for coupled-resonator networks, analytical computer-aided tuning (CAT) algorithms for microwave and millimeter-wave filters, and diplexers with applications in cellular base stations and satellites. He is also interested in modeling and optimization of passive RF components and computer-aided design techniques, such as the homotopy method, artificial neural networks, and machine learning techniques.

Zhou Jinzhu received his PhD degree from Xidian University, China in 2011. He is currently a professor with the State Key Laboratory of Electromechanical Integrated Manufacturing of High-performance Electronic Equipments, Xidian University. He is also the Director of the Department of Electronic Packaging and the Deputy Director of the Xi'an Key Laboratory of Intelligent Instrument and Packaging Test, Xidian University. He received the Outstanding Youth of Shaanxi Province in 2022. His research interests include microwave filter tuning, RF microsystem, smart skin antenna, and machine learning. He has published over 60 papers and holds 40 patents issued. Dr. Zhou received the National Science and Technology Award (2021 First Prize), the Science and Technology Progress Award of China Electronics Society (2022 First Prize), the Shaanxi Province Science and Technology Award (2015 First Prize), and the National Defense Science and Technology Award (2019 Second Prize). He also received four Best Paper Awards for the research of smart skin antenna and automatic microwave filter tuning in the International Conference of the 2010 IEEE International Conference on Mechatronics and Automation (ICMA), the Asia International Symposium on Mechatronics (AISM 2015), the AISM 2017, and the 2021 IEEE International Conference on Electronic Packaging Technology (ICEPT), respectively.

Shen Nan received his BS degree from Northwestern Polytechnical University, China in 2004 and MS degree in electromagnetic field and microwave technology from the same university in 2007. He is currently with ZTE Corporation, where his research focuses on filters, multiplexers, and antennas.

Wu Qingqiang received his BS degree from Xidian University, China in 2019, and MS degree in electromagnetic wave and microwave technology from the National Key Laboratory of Antennas and Microwave Technology, Xidian University in 2021. He is currently with ZTE Corporation, where his research focuses on filters and multiplexers.

New Member of ZTE Communications Editorial Board

Guo Yike is the Provost of the Hong Kong University of Science and Technology (HKUST), China; a Chair Professor in both the Department of Computer Science and Engineering and the Department of Electronic and Computer Engineering at HKUST; and also serves as the Director of the Hong Kong Generative AI Research and Development Center, China. He is a world-renowned computer scientist who has led several large-scale AI and data science research projects in China (including both Mainland and Hong Kong), the UK and other European countries. He was the Founding Director of the Data Science Institute at Imperial College London, UK, one of its seven Global Institutes, as well as the Vice President (Research and Development) at Hong Kong Baptist University, China. He is a Fellow of the Royal Academy of Engineering (FREng), a member of Academia Europaea (MAE), a Fellow of the Hong Kong Academy of Engineering Sciences (FHKEng), a Fellow of the Institute of Electrical and Electronics Engineers (FIEEE), a Fellow of the British Computer Society (FBCS), and a Fellow of Chinese Association for Artificial Intelligence (FCAAI).

Professor Guo was awarded the Outstanding Contribution Award of the 2022 Wu Wenjun Artificial Intelligence Science and Technology Award, China, which is considered to be the highest award for Chinese AI science and technology. In June 2025, Professor Guo was named "Leader of the Year 2024" in the Education/Professional/Technology and Innovation category from Sing Tao News Corporation, Hong Kong, China, for his transformative contributions to education and technological innovation in Hong Kong. In November of the same year, Professor Guo was elected as an international member of the Chinese Academy of Engineering (CAE) in recognition of his exceptional contributions to the Information and Electronics Engineering Division. The CAE is the nation's highest academic institution in engineering science and technology, and membership is considered the highest lifelong academic honor in the field.